

Ursolic acid treats renal tubular epithelial cell damage induced by calcium oxalate monohydrate via inhibiting oxidative stress and inflammation

Zhaohui Jia, Wensheng Li, Pan Bian, Liuyang Yang, Hui Liu, Dong Pan, and Zhongling Dou

Department of Urology, The First Affiliated Hospital and College of Clinical Medicine of Henan University of Science and Technology, Luoyang City, Henan Province, China

ABSTRACT

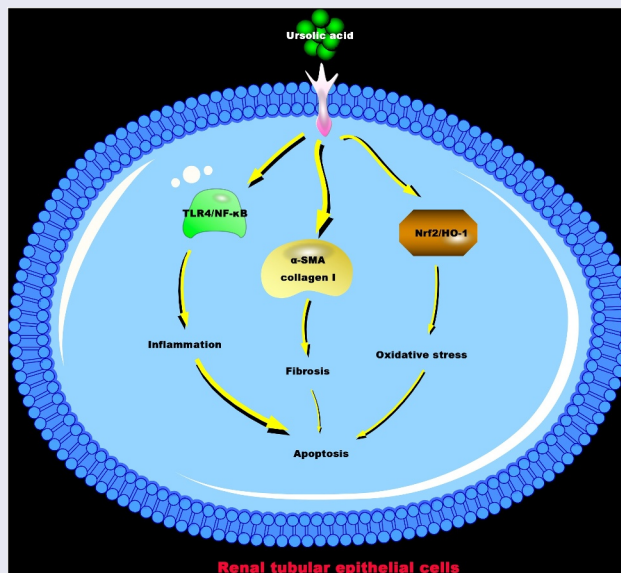
Ursolic acid (UA) has been proved to have antioxidant and anti-inflammatory effects. However, it is not clear whether it has a protective impact on kidney damage induced by crystals of calcium oxalate monohydrate (COM). This work aimed to make clear the potential mechanism of UA protecting COM-induced kidney damage. The results manifested that high- and low-dose UA reduced COM crystals in COM rats' kidney, down-regulated urea, creatinine, and neutrophil gelatinase-associated lipocalin (NGAL) levels in rat plasma, declined kidney tissue and HK-2 cell apoptosis, inhibited Bax expression but elevated Bcl-2 expression. Additionally, UA alleviated renal fibrosis in COM rats, repressed α -SMA and collagen I protein expressions in the kidney and COM rats' HK-2 cells, depressed COM-induced oxidative damage *in vivo* and *in vitro* via up-regulating Nrf2/HO-1 pathway, up-regulated SOD levels and reduced MDA levels, down-regulated TNF- α , IL-1 β , and IL-6 levels *in vivo* and *in vitro* via suppressing activation of TLR4/NF- κ B pathway. In summary, the results of this study suggest that COM-induced renal injury can be effectively improved via UA, providing powerful data support for the development of effective clinical drugs for renal injury in the future.

ARTICLE HISTORY

Received 1 June 2021
Revised 7 July 2021
Accepted 8 July 2021

KEYWORDS



Ursolic acid; crystals of calcium oxalate monohydrate; oxidative stress; inflammation; renal damage



1. Introduction

Kidney stone, a common kidney disease, due to lifestyle and diet and other reasons, features increasing global prevalence [1]. The most vital component of kidney stones is calcium oxalate

monohydrate (COM) crystals. Oxalate, one-end product of glyoxylate, amino acids, and carbohydrates metabolized in the liver [2], is mainly filtered and secreted through the glomeruli and renal tubules, finally excreted by the kidney. This

CONTACT Zhongling Dou  douzl8990@hotmail.com  Department of Urology, The First Affiliated Hospital and College of Clinical Medicine of Henan University of Science and Technology, Luoyang City, Henan Province 471003, China

© 2021 The Author(s). Published by Informa UK Limited, trading as Taylor & Francis Group.
This is an Open Access article distributed under the terms of the Creative Commons Attribution-NonCommercial License (<http://creativecommons.org/licenses/by-nc/4.0/>), which permits unrestricted non-commercial use, distribution, and reproduction in any medium, provided the original work is properly cited.

process is mediated by the SLC26A anion exchanger expressed in basolateral membrane [3]. Based on a great many studies, high-level oxalate or calcium oxalate crystals in the body can accelerate free radicals and inflammatory factors to produce in the kidney, causing kidney inflammation, oxidative stress, and even cell apoptosis [4–6]. Currently, there is still a lack of natural and safe inhibitors to depress renal calcium oxalate crystallization and alleviate kidney damage. Therefore, it is urgent to seek an effective inhibitor for renal calcium oxalate crystallization.

Ursolic acid (UA), a pentacyclic triterpene compound stems from the berries, fruits, leaves, and flowers of many medicinal plants. In Asia, it has been applied as an anti-inflammatory and hypoglycemic agent for centuries [7]. UA is available to suppress inflammation in various ways. Chen Z et al. reported that UA protects lipopolysaccharide-induced inflammation via inhibiting NLRP3 inflammatory nucleosomes [8]. Additionally, it also plays a protective role in neuroinflammation via depressing the activation of NF- κ B and I β 1 [9] and improve cell damage in the body via curbing oxidative stress. Samiver R et al. reported that UA relieves UVB radiation-induced oxidative stress in human dermal fibroblasts via dampening the production of reactive oxygen species (ROS) and lipid peroxidation, changing mitochondrial membrane potential, and regulating antioxidant pathway activity [10]. Additionally, UA mitigates intestinal oxidative stress in rat models of intestinal fibrosis [11]. Recent studies have revealed that UA improves lipopolysaccharide-induced acute kidney injury via blocking TLR4/MYD88 pathway [12]. Ma TK et al. also reported that UA lightens inflammation, oxidative stress, and apoptosis in diabetic nephropathy via regulating ARAP1/AT1R signaling pathway [13], indicating that ursolic acid may act actively in treating kidney diseases. In 2010, Hsu CL et al. found that a plant containing UA is able to treat kidney stones and dysuria [14]. Although previous studies have revealed that UA has ameliorative effects on various kidney injuries, it is ill-defined whether UA has a protective effect on oxalate-induced kidney injury and kidney stones.

Based on this, we hypothesized that UA had a therapeutic effect on oxalate-induced renal

tubular epithelial cell injury. In order to prove this hypothesis, the present study investigated the effects of UA on oxalate-induced fibrosis, oxidative stress, inflammation, and apoptosis of renal tubular epithelial cells *in vivo* and *in vitro*.

2. Methods

2.1. Animal model establishment

In total 8-week-old SFP-grade Sprague-Dawley (SD) rats from the Animal Laboratory of the First Affiliated Hospital and College of Clinical Medicine of Henan University of Science and Technology, were by randomly allocated into Control group, COM group, low-dose UA group (L-UA) and high-dose UA group (H-UA), six rats each. Except for Control group, all groups received 1% ethylene glycol and 2% 2 mL of ammonium chloride via gavage once a day. Meanwhile, the L-UA and H-UA groups were daily given 20 mg/kg and 40 mg/kg of UA via gavage, Control group receiving the same volume of distilled water via gavage each day. After 4 weeks, the rats were sacrificed through intraperitoneal injection of sodium pentobarbital (40 mg/kg) and their blood was taken from aorta. After being set aside for 2 h at room temperature, the blood received centrifugation at 4°C for 10 min to collect serum and store at –80°C for follow-up analysis. After death, some rat kidneys were quickly collected and fixed in 4% paraformaldehyde, and the remaining kidney tissue was stored at –80°C for subsequent analysis. All steps of animal experiments strictly followed the research ethics regulations of the First Affiliated Hospital and College of Clinical Medicine of Henan University of Science and Technology.

2.2. Hematoxylin-Eosin (HE) and Masson staining

HE and Masson staining were constructed as before [15]. The renal tissue fixed in 4% paraformaldehyde for another 24 h, was later fixed in paraffin to cut into continuous coronal sections (4 μ m), and deparaffinized in xylene. The sections were hydrated in gradient ethanol. Hematoxylin and Eosin (H&E) staining was applied to observe

the tissue structure. Based on the kit instructions, the sections were stained with Masson's trichrome stain (Solarbio), digital microscope cameras (DP12 SZX7, Olympus Corporation, Japan) applied to take images.

2.3. TdT-mediated dUTP-biotin nick end-labeling (TUNEL) staining

TUNEL staining was carried out as same as before [16]. TUNEL positive cells (green) and total cells (blue) were counted in five by random selected fields of each slide under fluorescence microscopes (Zeiss AxioVision, Germany) at 400 × magnification, and the apoptosis rate analyzed via Image Pro Plus 6.0 (Media Cybernetics, US.).

2.4. Immunohistochemistry

Immunohistochemical analysis was performed based on previous studies [17]. The sections were deparaffinized at 60°C for 1 h, washed twice in xylene for 10 min, and later rehydrated in descending alcohol series. After the antigen was recovered in microwave for 12 min, the tissue was combined with primary antibodies Bax (ab173026; 1:1000; Abcam), Bcl-2 (ab182858; 1:1000; Abcam), α -SMA (A2547, 1:1000, MilliporeSigma), collagen I (ab34710, 1:1000, Abcam), MYD88 (4283, 1:1000, Cell Signaling Technology), TLR4 (sc-293,072, 1:1000, Santa Cruz Biotechnology), Nrf2 (ab62352, 1:1000, Abcam), HO-1 (ab13248, 1:1000, Abcam) to incubate together. After 16 h, the tissue with goat anti-rabbit immunoglobulin G (IgG) secondary antibody conjugated with horseradish peroxidase was incubated for 1 h (1:2,000, catalog number TA130024, OriGene Technologies, Inc.), and later stained with diaminobenzidine for 5 min at room temperature, digital microscope cameras applied to take images.

2.5. Cell culture

Renal tubular epithelium (HK-2 cells) bought from American Type Cell Collection (CRL-2190, ATCC, France), were cultured in Dulbecco's modified Eagle's medium/Ham's F12 (DMEM/F12, 1:1) with 10% fetal calf serum (FCS), 2% antibiotic-

antifungal drugs, at 37°C with 5% CO₂, stored in a 25 cm² flask (Gibico, US) for cell monolayer.

2.6. UA toxicity testing

Cytotoxicity was tested via 3-(4, 5-dimethylthiazol-2-yl)-2, 5-diphenyltetrazolium bromide (MTT) assay [18]. The cells transferred to 96-well plates (1 × 10⁵/well) were exposed to serum- and pyruvate-free medium. Aiming to obtain optimal UA concentration, HK-2 cells were exposed to 0, 2.5, 5, 7.5, and 10 μ M UA. After 24 h, followed by MTT cell proliferation and cytotoxicity assay kit (Nanjing Jiancheng Biotechnology Co., Ltd.) to evaluate cell viability via measuring the absorbance at 570 nm.

2.7. Cell grouping

The cells were allocated into four groups: Control group (HK-2 cells not exposed to any reagent); COM group (HK-2 cells exposed to 200 mg/L COM crystals and 2 mmol/L oxalate); L-UA and H-UA groups (2.5 μ M and 5 μ M UA added to medium, respectively). After 30 min-incubation, HK-2 cells were exposed to 200 mg/L COM crystals and 2 mmol/L oxalate. After 24 h, the medium and cells were for subsequent testing.

2.8. Enzyme-linked immunosorbent assay (ELISA)

In reference to the instructions, malondialdehyde (MDA), superoxide dismutase (SOD), interleukin (IL)-1 β , tumor necrosis factor (TNF)- α , and IL-6 levels in rat kidney tissue and HK-2 cells, Na⁺/K⁺ ATPase activity in HK-2 cells, as well as creatinine, urea and NGAL levels in rat serum were detected, all ELISA kits were purchased from Nanjing Jiancheng Biotechnology Company.

2.9. Flow cytometry

The cells were digested with trypsin, analyzed via flow cytometry and APC Annexin V/propidium iodide (PI) apoptosis detection kit (BioLegend, US), washed with phosphate buffered saline (PBS), suspended in AV binding buffer (BioLegend), and adjusted to 1 × 10⁵ cells/mL,

and later stained with AV/PI Detection Reagent for 30 min in the dark. Cell apoptosis was detected via FACSCalibur flow cytometer (BD).

2.10. Reverse transcription quantitative polymerase chain reaction (RT-qPCR)

RT-qPCR was applied according to previous methods [19]. Total RNA isolated from cells via TRIzol reagent (Invitrogen) received reverse transcription via M-MLV reverse transcriptase (Invitrogen) to synthesize complementary DNA (cDNA). The RT-qPCR analysis was performed on ABI Prism 7500 fast real-time PCR system (Applied Biosystems, US) via Power SYBR Green Master Mix (Applied Biosystems). Relative expression was evaluated via $2^{-\Delta\Delta C_t}$ method, GAPDH as an internal reference. The primer sequence is in Table 1.

2.11. Western blot

Cells were lysed via RIPA lysis buffer (Beyotime, China), and total protein concentration was measured via Pierce BCA protein analysis kit (Pierce, US). After elution in sample loading buffer (Beyotime) and separation via SDS-PAGE, the samples were transferred to PVDF films at a constant current of 200 mA. The films blocked with 5% skim milk in Tris-buffered saline Tween (TBST) at room temperature, and the primary antibodies GAPDH (2118, Cell Signaling Technology, 1:1000), p-NF- κ B (3033, 1:1000, Cell Signaling Technology), NF- κ B (8242, 1:1000, Cell Signaling Technology), TLR4 (sc-293,072, 1:1000, Santa Cruz Biotechnology), Nrf2 (ab62352, 1:1000, Abcam), HO-1 (Ab13248, 1:1000, Abcam), α -SMA (A2547, 1:1000, MilliporeSigma), collagen I (ab34710, 1:1000, Abcam) were incubated. After being washed in triplicate with TBST, they were cultured with secondary antibody (goat anti-rabbit IgG, ab6721,

1:5000) in an incubator for 1.5 h at room temperature. Later being washed again with TBST 3 times, the films were treated with ECL Plus substrate bought from Life Technologies Corporation (Gaithersburg, US) to detect protein signals. The image acquisition and analysis system of Lab Works version 4.5 software (SIL Technologies, Inc., IL, US) were applied to detect and quantify the immunoreactive signal of protein bands.

2.12. Data analysis

The experimental findings were shown as mean \pm standard deviation (SD), via SPSS 22 software for data analysis, including Student's t-test and one-way analysis of variance (ANOVA). Via Tukey's test to perform multiple variance correction on samples, the difference among experimental groups is considered significant when $P < 0.05$. All experiments were biologically duplicated.

3. Results

3.1. UA reduced COM-induced pathological damage to the kidney

Aiming to probe into the protective impact of UA on COM rats' kidney, the pathological morphology of their kidneys was examined via HE staining. There was no crystal deposition in Control, L-UA, and H-UA groups, but with obvious deposition in COM group (Figure 1a). Additionally, we examined the influence of UA on renal function indicators. Compared with Control group, plasma urea, creatinine, and NGAL levels in COM rats increased signally (Figure 1b), whereas high- and low-dose UA signally reversed them. Later, the study further examined the protective impact of UA on COM-induced HK-2 cell damage via *in vitro* experiments. We first examined the toxic effect of UA on HK-2 cells exposed to different UA concentrations to check cell viability. UA at 2.5 and 5 μ M was not toxic to HK-2 cells, while at 7.5 and 10 μ M decreased cell viability in a dose-dependent manner (Figure 1c). HK-2 cells pretreated with 2.5 and 5 μ M UA were exposed to COM for 24 h, finding that (Figure 1d) the cell viability in COM group was signally lower than that in Control group, whereas visually lower than

Table 1. qRT-PCR primer sequences.

	primer sequences (5' – 3')
GAPDH	Forward: 5'-CCTCGTCTCATAGACAAGATGGT-3' Reserse: 5'-GGGTAGAGTCATACTGGAACATG-3'
Bcl-2	Forward: 5'- CTGGTGGACAACATCGCTCTG –3' Reserse: 5'- GGTCTGCTGACCTCACTTGTG –3'
Bax	Forward: 5'- GGATCGAGCAGAGAGGATGG –3' Reserse: 5'- TGGTGAGTGAGGCAGTGAGG –3'

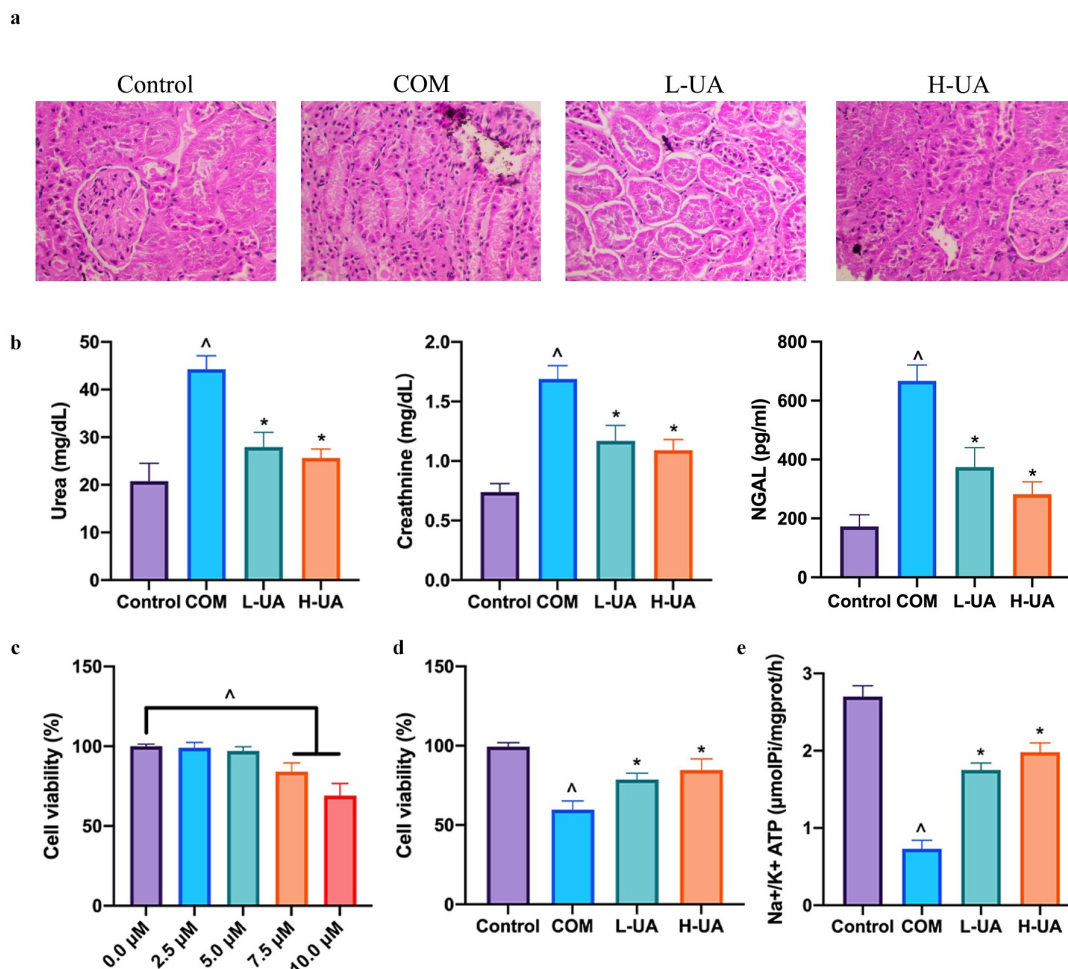


Figure 1. UA reduced COM-induced pathological damage to the kidney.

Note: A: HE staining checked the pathological conditions of all rats' kidney tissues; B: ELISA detected plasma urea, creatinine, and NGAL levels in each group; C: MTT detected HK-2 cell viability after receiving different UA concentrations; D: MTT detected HK-2 cell viability in each group; E: ELISA detected Na⁺/K⁺ ATPase activity in HK-2 cells in each group; the values were mean ± SD (B, n = 6; CE, n = 3); one-way ANOVA was applied to calculate the significance of each group; the variance was corrected via Tukey's test; vs Control group, [^]P < 0.05; vs COM group, ^{*}P < 0.05.

that in L-UA and H-UA groups in a dose-dependent manner. Additionally, Na⁺/K⁺ ATPase level in COM group was significantly lower than that in Control group, whereas observably lower than those in L-UA and H-UA groups significantly (Figure 1e). (Figure 1)

3.2. UA attenuated COM-induced HK-2 cell apoptosis

Next, the study exploited the impact of UA on COM-induced HK-2 cell apoptosis. TUNEL staining findings revealed that the number of TUNEL-positive cells in COM group was significantly elevated

with contrast to that in Control group, and high- and low-dose UA could visually reduce the number (Figures 2a and 2b). Later, the impact of UA on Bax and Bcl-2 apoptosis proteins in COM rats were examined via immunohistochemistry. Compared with Control group, Bax expression in COM group was apparently elevated whereas Bcl-2 expression was distinctly reduced (Figure 2c). High- and low-dose UA reversed Bax and Bcl-2 expressions in COM rats, which was further verified *in vitro*. Flow cytometry findings revealed that after 24-h exposure to COM, HK-2 cell apoptotic rate was up-regulated visually (Figure 2d), but after pretreatment with low- and high-dose

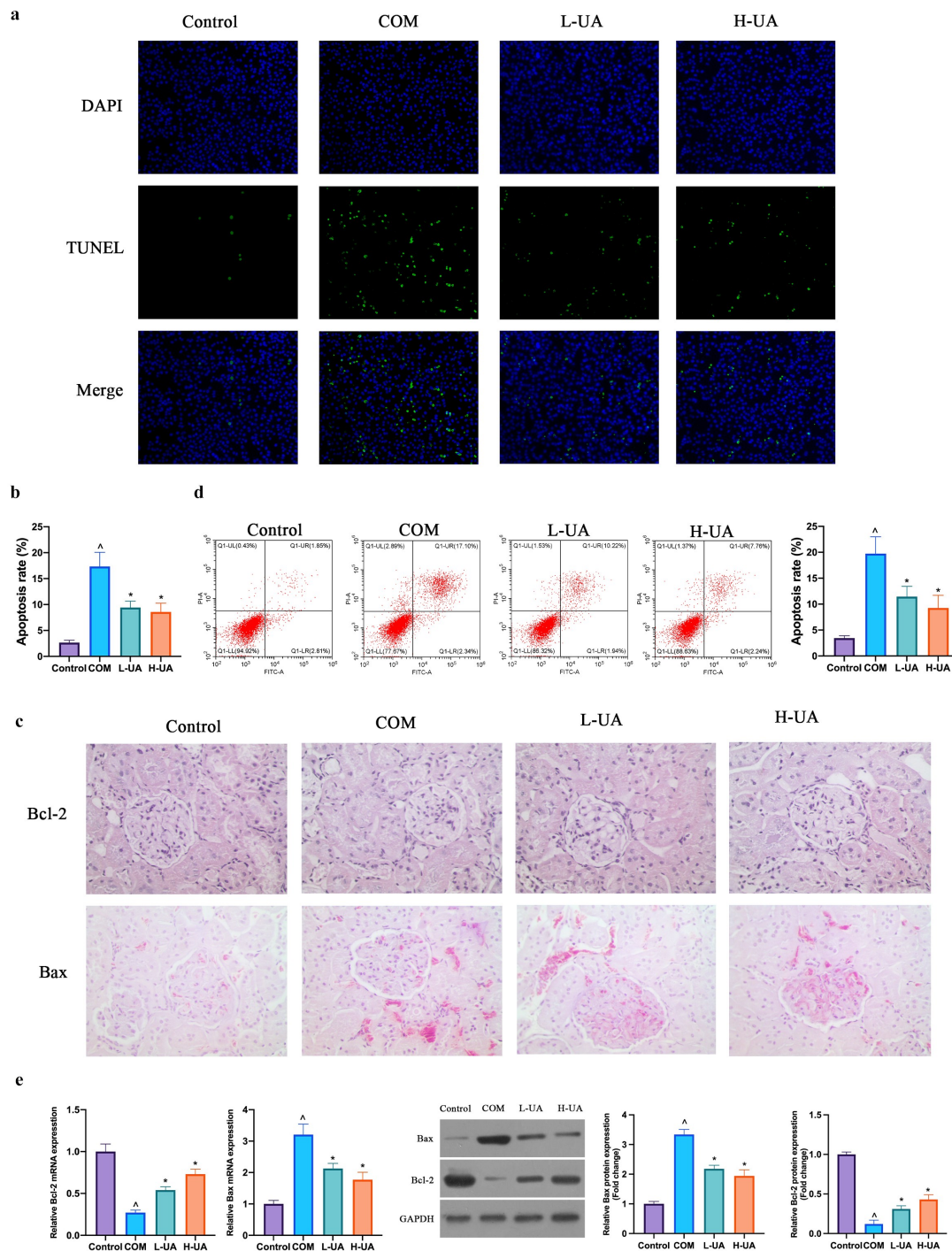


Figure 2. UA reduced COM-induced HK-2 cell apoptosis.

Note: A & B: TUNEL staining tested HK-2 cell apoptosis rate in each group; C: Immunohistochemistry checked Bcl-2 and Bax protein expressions in each group; D: Flow cytometry checked HK-2 cell apoptosis rate in each group; E: RT-qPCR and western blot checked Bcl-2 and Bax expressions in HK-2 cells in each group; the values were mean \pm SD (B, n = 6; DE, n = 3); one-way ANOVA was applied to calculate the significance of each group; the variance was corrected via Tukey's test; vs Control group, $\wedge P < 0.05$; vs COM group, $*P < 0.05$.

UA, the apoptotic rate in COM group was observably reduced. Additionally, RT-qPCR and western blot findings revealed that, in comparison with Control group, Bcl-2 expression in COM

group was evidently reduced and Bax expression was markedly elevated (Figure 2e). Low- and high-dose UA pretreatment obviously alleviated this phenomenon. (Figure 2)

3.3. UA reduced COM-induced renal fibrosis

The degree of renal fibrosis in each group was examined via Masson staining. The degree in Control group was very low, with almost no blue collagen fibers stained by Masson's staining (Figure 3a), the degree in COM group was high, with blue collagen fibers in great number, and the degree in L-UA and H-UA groups was manifest lower by contrast with that in COM group, with greatly reduced blue collagen fibers. Later, α -SMA and collagen I expressions in rats' kidney tissues was examined via immunohistochemistry and western blot. α -SMA and Collagen I protein expressions in COM group was overtly up-regulated by contrast with that in Control group, while L-UA and H-UA treatment visually reduced them in COM rats (Figures 3b and 3c). Additionally, this finding was further verified in HK-2 cells (Figure 3d). (Figure 3)

3.4. UA protected the kidney from COM-induced oxidative damage

Next, the study probed into the effect of UA on COM-induced renal oxidative stress. COM increased MDA level in COM rats and decreased SOD level (Figure 4a), while high- and low-dose UA obviously reduced MDA level in COM rats and up-regulated SOD level. Additionally, Nrf2/HO-1 axis is an essential pathway for anti-oxidative stress in the body. The study found that COM apparently reduced Nrf/HO-1 protein expression in COM rats, but high- and low-dose UA could restore it (Figures 4b and 4c). In *in vitro* experiments, after COM exposure, MDA level in HK-2 cells elevated visually, whereas SOD level decreased signally. After pretreatment with high- and low-dose UA, MDA level was evidently reduced and SOD level was restored (Figure 4d), finding that COM exposure inhibited Nrf2/HO-1 protein expression in HK-2 cells, while in COM group pretreated with high- and low-dose UA, Nrf2/HO-1 protein expression was manifest elevated (Figure 4e). (Figure 4)

3.5. UA protected the kidney from COM-induced renal inflammatory damage

The study explored the effect of UA on COM-induced renal inflammation. COM signally elevated TNF- α , IL-1 β , and IL-6 levels in rats' kidney

tissues, whereas high- and low-dose UA visually reduced them (Figure 5a). TLR4/NF- κ B axis has been found to promote various inflammatory factors expressions in the body, finding that COM signally elevated MYD88, TLR4 protein, and phosphorylated NF- κ B protein expressions in rat kidney tissue, whereas high- and low-dose UA could apparently decrease them (Figure 5b, c). Additionally, in *in vitro* experiments the study found that COM exposure signally elevated TNF- α , IL-1 β , and IL-6 levels in HK-2 cells, while UA pretreatment distinctly reduced them after COM exposure (Figure 5d). After COM exposure, TLR4 and phosphorylated NF- κ B protein expressions in HK-2 cells elevated markedly, whereas after UA pretreatment, they in COM group were signally inhibited (Figure 5e). (Figure 5)

4. Discussion

The study found that UA protects the kidney from COM-induced damage via inhibiting renal fibrosis, apoptosis, inflammation, and oxidative stress in *in vivo* and *in vitro* models.

In this study, it was the first time to demonstrate that UA treatment could reduce COM-induced renal crystal aggregation, indicating the large potential of UA on amelioration of kidney stones and urinary tract obstruction. Many studies have manifested that plant extracts are capable of reducing kidney stones, such as dietary polyphenolic caffeic acid [20], astragalus polysaccharide [21], and gambogus extract [22]. However, the clinical efficacy of plenty of plant extracts in all kinds of diseases is limited by bioavailability and solubility, including UA. At present, scientists improve the bioavailability and solubility of UA by means of chemical modification [23]. Therefore, UA can be applied as a potential clinical drug for the treatment of kidney stones in the future. Although the study has demonstrated that UA could decline COM-induced renal crystal deposition, the effect of 40 mg/kg UA on normal rats is still unclear, which needs to be examined in future work. Besides, a positive drug group was not set in this study, which is the limitation of this study. After treating COM model rats with high- and low-dose UA, the plasma creatinine level in COM rats was manifest reduced. It is known that

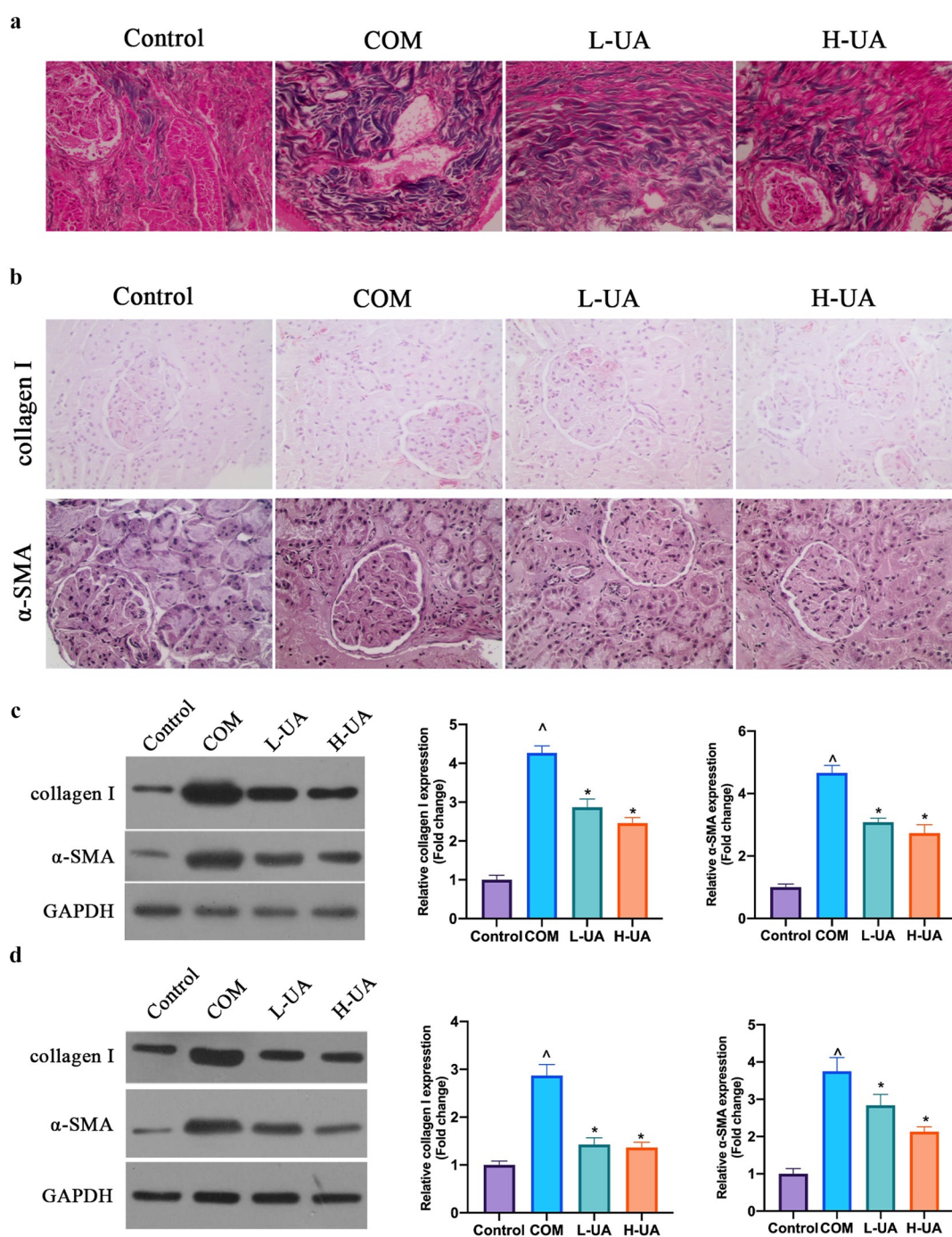


Figure 3. UA reduced COM-induced renal fibrosis.

Note: A: Masson staining given to each group; B: Immunohistochemistry examined α -SMA and collagen I protein expressions in each group; C: Western blot checked α -SMA and collagen I protein expressions in HK-2 cells of each group; the values were mean \pm SD (C, n = 6; D, n = 3); one-way ANOVA was applied to calculate the significance of each group; the variance was corrected via Tukey's test; vs Control group, [^] $P < 0.05$; vs COM group, * $P < 0.05$.

creatinine is an essential indicator for evaluating glomerular damage, because its content in plasma depends on many factors, like glomerular filtration rate, renal tubular secretion rate, and urine volume [24]. Additionally, the study also found that urea

level in COM rats' plasma elevated, which was reversed via UA intervention. Increased urea and creatinine levels in COM rats may be due to excessively accumulated COM crystals in kidney tissue, whereas reduced plasma creatinine and urea levels

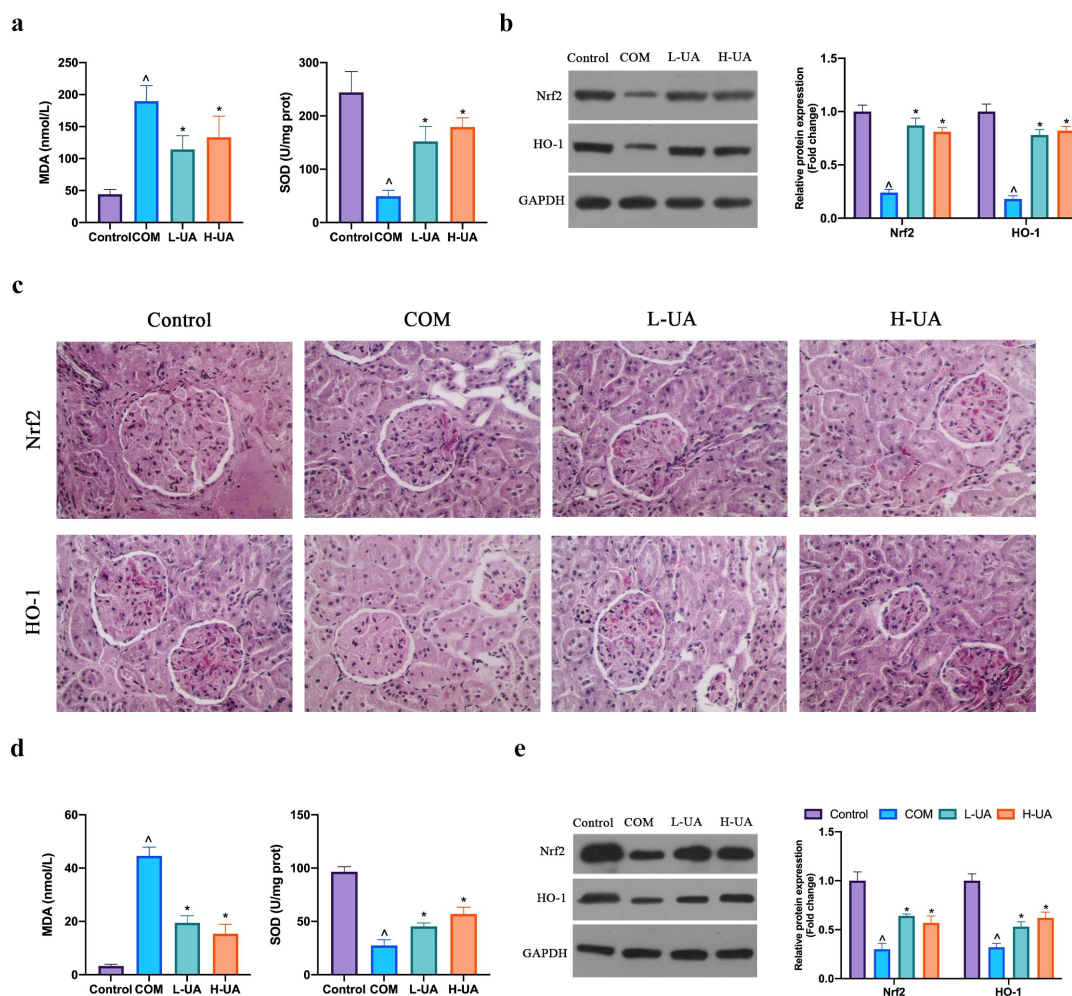


Figure 4. UA protected the kidney from COM-induced oxidative damage.

Note: A: ELISA detected MDA and SOD levels in each group; B: Western blot detected Nrf2/HO-1 protein expression in each group; C: Immunohistochemistry detected Nrf2/HO-1 protein expression; D: ELISA detected MDA and SOD levels in each group; E: Western blot detected Nrf2/HO-1 protein expression in each group; the values were mean \pm SD (AB, $n = 6$; DE, $n = 3$); one-way ANOVA was applied to calculate the significance of each group; the variance was corrected via Tukey's test; vs Control group, $^{\Delta}P < 0.05$; vs COM group, $*P < 0.05$.

via UA may impose an impact via inhibiting COM crystals in kidney tissue. What's more, NGAL was declined via UA. In the early stages of kidney injury, NGAL in serum is distinctly elevated, prompting that UA plays an important role in the early stages of kidney damage [25]. Importantly, UA treatment signally elevated Na^+/K^+ ATPase activity in HK-2 cells. Sodium, potassium, and mercury are vital for maintaining intracellular environment. Based on previous studies, oligomeric proanthocyanidins up-regulates Na^+/K^+ ATPase activity to repress oxidative stress resulting from COM crystals on HK-2 cells [26], whereas UA features a similar impact.

Renal crystal aggregation has key connection with renal fibrosis. In reference to previous studies, UA is available to suppress TGF- β 1-induced renal fibrosis via depressing α -SMA, snail, slug, and other protein expressions [27]. Renal fibrosis is the final universal pathological feature of various chronic kidney diseases, which is closely related to inflammation, oxidative damage, and apoptosis [28,29]. These studies have revealed that COM induces obvious renal fibrosis as well, which is consistent with our findings [30]. A great many studies have revealed that α -SMA and collagen I proteins acts pivotally in renal interstitial fibrosis and

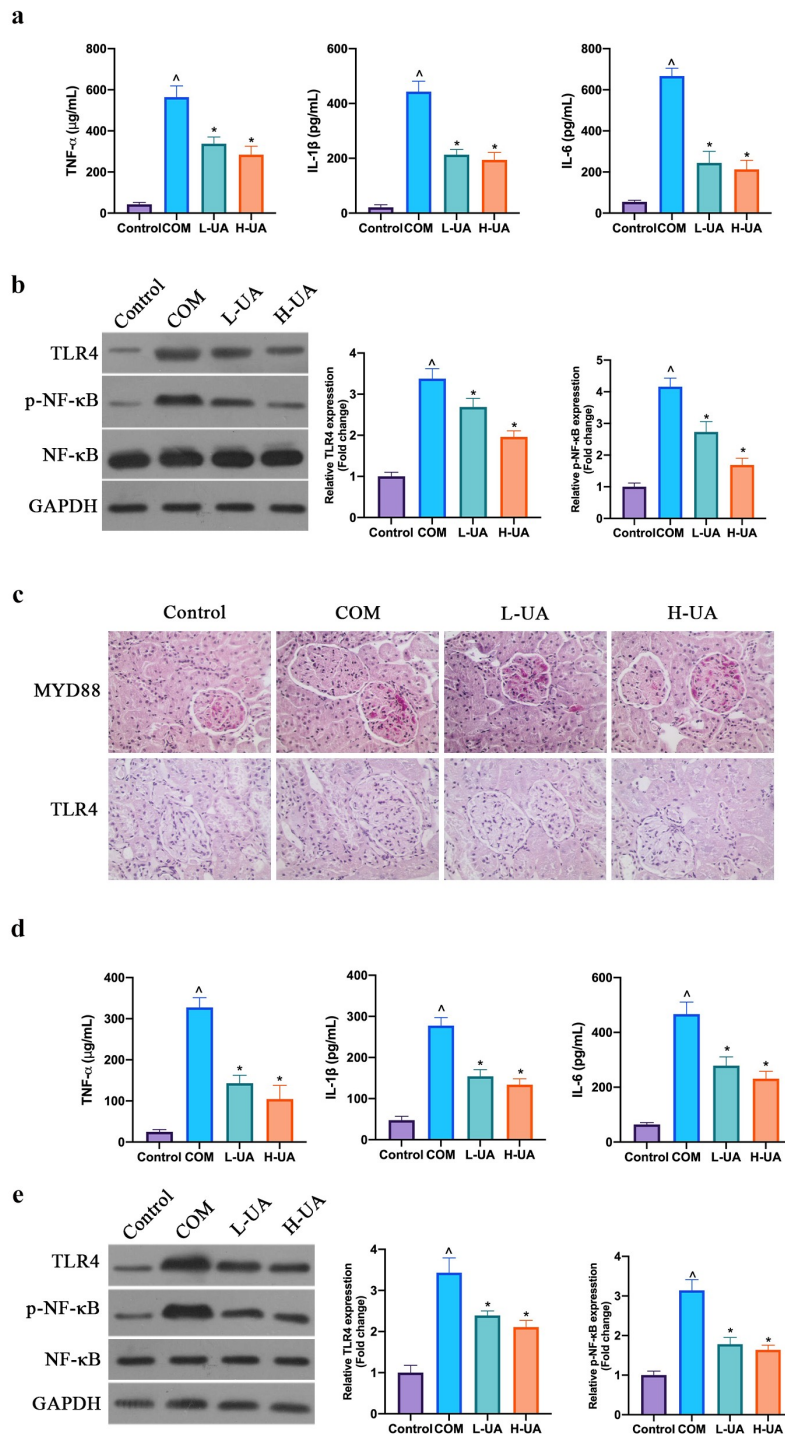


Figure 5. UA protected the kidney from COM-induced renal inflammation damage.

Note: A: ELISA detected TNF- α , IL-1 β , and IL-6 levels in each group; B: Western blot detected TLR4 and phosphorylated NF- κ B protein expressions in each group; C: Immunohistochemistry examined MYD88 and TLR4 protein expressions in each group; D: ELISA tested TNF- α , IL-1 β , and IL-6 levels in each group; E: Western blot detected TLR4 phosphorylated NF- κ B protein expressions in HK-2 cells of each group; the values were mean \pm SD (AB, n = 6; DE, n = 3); one-way ANOVA was applied to calculate the significance of each group; the variance was corrected via Tukey's test; vs Control group, $^{\wedge}P < 0.05$; vs COM group, $*P < 0.05$.

epithelial–mesenchymal transition [31,32]. In this work, we found that high- and low-dose UA are available to depress α -SMA and collagen

I protein expressions *in vivo* and *in vitro*, helping to improve COM-induced renal fibrosis, thus cutting down Com crystal deposit.

Nrf2 is a member of CNC-bZIP (cap'collar-basic leucine zipper) transcription activator family. After forming a heterodimer with the Neh1 domain and Maf protein, it combines with antioxidant reaction element (ARE) to regulate the activity of target genes like SOD, CAT, and phase II detoxification enzymes [33]. HO-1 is among the phase II detoxification enzymes, and the downstream signal pathways it triggers have antioxidant effects on various organs [34]. Based on previous studies, UA is available to regulate Nrf2 pathway in all types of diseases, such as cancer and emphysema [35,36]. The study found that UA increased SOD level and reduced MDA level in COM models *in vivo* and *in vitro* via up-regulating Nrf2/HO-1 expression, and repressing COM-induced oxidative stress. It is known that oxidative stress is a key mechanism of COM-induced kidney damage. Excessive ROS is available to activate NF- κ B inflammation signaling pathway and induce cell apoptosis [37]. Previous studies have revealed that inhibiting ROS production alleviates COM-induced inflammation in renal tubular epithelial cells. This work found that UA repressed TLR4/NF- κ B pathway to impede COM-induced renal inflammation. Whether this effect is achieved through regulating ROS production needs further study.

5. Conclusion

To sum up, our findings indicate that UA is available to reduce COM crystallization in renal tissue and knockdown COM-induced renal cell apoptosis, oxidative damage, inflammation, and renal fibrosis via regulating Nrf2/HO-1 oxidative stress signaling pathway, TLR4/NF- κ B inflammatory signaling pathway, as well as α -SMA and collagen I protein expressions. This provides data support for UA as an effective drug for treating kidney stones later.

Disclosure statement

No potential conflict of interest was reported by the author(s).

Funding

National Natural Science Foundation of China (grant no. 81800628) Henan Natural Science Foundation (grant no. 162300410106).

References

- [1] Khan S. Role of renal epithelial cells in the initiation of calcium oxalate stones. *Nephron Exp Nephrol.* 2004;98(2):e55–60.
- [2] John K, Dean GA, Michael FC, et al. Metabolism of primed, constant infusions of [1,2-¹³C₂] glycine and [1-¹³C₁] phenylalanine to urinary oxalate. *Metabolism.* 2011;60(7):950–956. .
- [3] Robijn S, Hoppe B, Vervaeck BA, et al. Hyperoxaluria: a gut-kidney axis? *Kidney Int.* 2011;80(11):1146–1158. .
- [4] Jiannan L, Kelaier Y, Yinshan J, et al. H3 relaxin protects against calcium oxalate crystal-induced renal inflammatory pyroptosis. *Cell Prolif.* 2020;53(10):e12902.
- [5] Larissa DA, Juliana MCP, Mariana CDP, et al. Sodium oxalate-induced acute kidney injury associated with glomerular and tubulointerstitial damage in rats. *Front Physiol.* 2020;11:1076.
- [6] Zizhi L, Linna C, Xiuli R, et al. Modulation of rat kidney stone crystallization and the relative oxidative stress pathway by green tea polyphenol. *ACS Omega.* 2021;6(2):1725–1731. .
- [7] Liu J. Pharmacology of oleanolic acid and ursolic acid. *J Ethnopharmacol.* 1995;49(2):57–68.
- [8] Zixi C, Qiaoli L, Zhaowei Z, et al. Ursolic acid protects against proliferation and inflammatory response in LPS-treated gastric tumour model and cells by inhibiting NLRP3 Inflammasome activation. *Cancer Manag Res.* 2020;12:8413–8424.
- [9] Rai SN, Zahra W, Singh SS, et al. Anti-inflammatory activity of ursolic acid in MPTP-induced parkinsonian mouse model. *Neurotox Res.* 2019;36(3):452–462. .
- [10] Ramachandran S, Rajendra PN, Umadevi S, et al. Inhibitory effect of ursolic acid on ultraviolet B radiation-induced oxidative stress and proinflammatory response-mediated senescence in human skin dermal fibroblasts. *Oxid Med Cell Longev.* 2020;2020:1246510.
- [11] Wang Z, Dakai G, Jie J, et al. Protective effect of ursolic acid on the intestinal mucosal barrier in a rat model of liver fibrosis. *Front Physiol.* 2019;10:956.
- [12] Jun Z, Haoyi Z, Zhongguo S, et al. Ursolic acid exhibits anti-inflammatory effects through blocking TLR4-MyD88 pathway mediated by autophagy. *Cytokine.* 2019;123:154726.
- [13] Tian-Kui M, Li X, Ling X, et al. Ursolic acid treatment alleviates diabetic kidney injury by regulating the ARAP1/AT1R signaling pathway. *Diabetes Metab Syndr Obes.* 2019;12:2597–2608.
- [14] Hsu CL, Hong BH, Yu YS, et al. Antioxidant and anti-inflammatory effects of Orthosiphon aristatus and its bioactive compounds. *J Agric Food Chem.* 2010 Feb 24;58(4):2150–2156.
- [15] Du X, Tao Q, Du H, et al. Tengdan capsule prevents hypertensive kidney damage in shr by inhibiting periostin-mediated renal fibrosis. *Front Pharmacol.* 2021;12:638298.

- [16] Kim JH, Jeong SJ, Kim B, et al. Melatonin synergistically enhances cisplatin-induced apoptosis via the dephosphorylation of ERK/p90 ribosomal S6 kinase/heat shock protein 27 in SK-OV-3 cells. *J Pineal Res.* **2012** Mar;52(2):244–252.
- [17] Emre C, Do KV, Jun B, et al. Age-related changes in brain phospholipids and bioactive lipids in the APP knock-in mouse model of Alzheimer's disease. *Acta Neuropathol Commun.* **2021** Jun 29;9(1):116.
- [18] Daniyal M, Liu Y, Yang Y, et al. Anti-gastric cancer activity and mechanism of natural compound "Heilaohulignan C" isolated from *Kadsura coccinea*. *Phytother Res.* **2021** Jun 21. DOI:10.1002/ptr.7114.
- [19] Yang C, Shi J, Wang J, et al. Circ_0006988 promotes the proliferation, metastasis and angiogenesis of non-small cell lung cancer cells by modulating miR-491-5p/MAP3K3 axis[J]. *Cell cycle (Georgetown, Tex.)*, **2021**, 20(13):1334–1346
- [20] Yasir F, Wahab AT, Choudhary MI. Protective effect of dietary polyphenol caffeic acid on ethylene glycol-induced kidney stones in rats. *Urolithiasis.* **2018** Apr;46(2):157–166.
- [21] Fan QX, Gong SQ, Hong XZ, et al. Clinical-grade *Garcinia cambogia* extract dissolves calcium oxalate crystals in *Drosophila* kidney stone models. *Eur Rev Med Pharmacol Sci.* **2020** Jun;24(11):6434–6445.
- [22] Huang F, Sun XY, Ouyang JM. Preparation and characterization of selenized *Astragalus* polysaccharide and its inhibitory effect on kidney stones. *Mater Sci Eng C Mater Biol Appl.* **2020** May;110:110732.
- [23] Mlala S, Oyedeji AO, Gondwe M, et al. Its derivatives as bioactive agents. *Molecules.* **2019** Jul 29;24(15):15.
- [24] Moran S, Myers B. Course of acute renal failure studied by a model of creatinine kinetics. *Kidney Int.* **1985**;27(6):928–37.
- [25] Shang W, Wang Z. The Update of NGAL in acute kidney injury. *Curr Protein Pept Sci.* **2017**;18(12):1211–1217.
- [26] Shuo W, Peng D, Ning Z, et al. Oligomeric proanthocyanidins protect against HK-2 cell injury induced by oxalate and calcium oxalate monohydrate crystals. *Urolithiasis.* **2016**;44(3):203–210. .
- [27] Xu CG, Zhu XL, Wang W, et al. Ursolic acid inhibits epithelial-mesenchymal transition in vitro and in vivo. *Pharm Biol.* **2019**;57(1):169–175. .
- [28] Chen H, Fan Y, Jing H, et al. Emerging role of lncRNAs in renal fibrosis. *Arch Biochem Biophys.* **2020**;692:108530.
- [29] Fan Y, Chen H, Huang Z, et al. Emerging role of miRNAs in renal fibrosis. *RNA Biol.* **2020**;17(1):1–12. .
- [30] Yueyan L, Rui Z, Guofeng X, et al. Generation and characterization of a novel rat model of primary hyperoxaluria type 1 with a nonsense mutation in alanine-glyoxylate aminotransferase gene. *Am J Physiol Renal Physiol.* **2021.** 320(3): F475-F484.
- [31] Mengkui S, Wei Z, Fei Y, et al. MicroRNA-302b mitigates renal fibrosis via inhibiting TGF- β /Smad pathway activation. *Braz J Med Biol Res = Rev Bras Pesqui Med Biol.* **2021**;54(3):e9206.
- [32] Zhou Y, Chai P, Wang J, et al. Wingless/int-1 induced secreted protein-1: a new biomarker for renal fibrosis. *J Biol Regul Homeost Agents.* **2021**;35(1):97-103.
- [33] Agnieszka L, Milena D, Elzbieta P, et al. Role of Nrf2/HO-1 system in development, oxidative stress response and diseases: an evolutionarily conserved mechanism. *Cell Mol Life Sci.* **2016**;73(17):3221–3247. .
- [34] Can AA, Mehmet T, Armagan H, et al. Taurine ameliorates neuropathy via regulating NF- κ B and Nrf2/HO-1 signaling cascades in diabetic rats. *Food Chem Toxicol.* **2014**;71:116–121.
- [35] Lin L, Yin Y, Hou G, et al. Ursolic acid attenuates cigarette smoke-induced emphysema in rats by regulating PERK and Nrf2 pathways. *Pulm Pharmacol Ther.* **2017**;44:111–121.
- [36] Chao W, Limin S, Chengyue Z, et al. Histone methyltransferase setd7 regulates Nrf2 signaling pathway by phenethyl isothiocyanate and ursolic acid in human prostate cancer cells. *Mol Nutr Food Res.* **2018**;62(18):e1700840. .
- [37] Shuai Z, Fan C, Qiliang Y, et al. Reactive oxygen species interact with NLRP3 inflammasomes and are involved in the inflammation of sepsis: from mechanism to treatment of progression. *Front Physiol.* **2020**;11:571810. .